α-Melanocyte-related tripeptide, Lys-D-Pro-Val, ameliorates endotoxin-induced nuclear factor κB translocation and activation: evidence for involvement of an interleukin-1β$^{193–195}$ receptor antagonism in the alveolar epithelium

John J. E. HADDAD*[1], Ryszard LAUTERBACH†, Nayef E. SAADÉ‡§, Bared SAFIEH-GARABEDIAN‖ and Stephen C. LAND*

*Oxygen Signalling Group, Centre for Research into Human Development, Tayside Institute of Child Health, Faculty of Medicine, Ninewells Hospital and Medical School, University of Dundee, Dundee DD1 9SY, Scotland, U.K., †Department of Neonatology, Jagiellonian University Medical College, PL-31-501 Cracow, Kopernika 23, Poland, ‡Department of Human Morphology, Faculty of Medicine, American University of Beirut, P.O. Box 11-0236, Beirut, Lebanon, §Department of Physiology, Faculty of Medicine, American University of Beirut, P.O. Box 11-0236, Beirut, Lebanon, and ‖Department of Biology, Faculty of Arts and Sciences, American University of Beirut, P.O. Box 11-0236, Beirut, Lebanon

The potential anti-inflammatory role of α-melanocyte-stimulating hormone (α-MSH)-related tripeptide, lysine^{11}-D-proline-valine^{13} (KDPV), an analogue of interleukin (IL)-1β$^{193–195}$ and an antagonist of IL-1β/prostaglandin E_2, is not well characterized in the alveolar epithelium. In a model of foetal alveolar type II epithelial cells *in vitro*, we showed that lipopolysaccharide endotoxin (LPS) differentially, but selectively, induced the nuclear subunit composition of nuclear factor κB_1 (NF-κB_1) (p50), RelA (p65) and c-Rel (p75), in parallel to up-regulating the DNA-binding activity (supershift indicating the presence of the p50–p65 complex). LPS accelerated the degradation of inhibitory κB-α (IκB-α), accompanied by enhancing its phosphorylation in the cytosolic compartment but not in the nucleus. KDPV suppressed, in a dose-dependent manner, the nuclear localization of p50, p65 and p75, an effect that led to the subsequent inhibition of NF-κB activation. Interleukin-1 receptor antagonist (IL-1ra) decreased the nuclear abundance of p50, p65 and p75, and subsequently depressed the DNA-binding activity induced by LPS. Analysis of the mechanism involved in the KDPV- and IL-1ra-mediated inhibition of NF-κB nuclear localization revealed a reversal in IκB-α phosphorylation and degradation, followed by cytosolic accumulation. LPS induced endogenous IL-1β biosynthesis in a time-dependent manner; the administration of exogenous recombinant human interleukin 1 (rhIL-1) resulted in a dose-dependent activation of NF-κB. KDPV and IL-1ra abrogated the effect of rhIL-1. Pretreatment with the non-steroidal anti-inflammatory drug (NSAID) indomethacin, an inhibitor of cyclo-oxygenase, blocked the LPS-induced activation of NF-κB. These results indicate the involvement of prostanoid-dependent (NSAID-sensitive) and IL-1-dependent (IL-1ra-sensitive) mechanisms mediating LPS-induced NF-κB translocation and activation, a pathway that is regulated, in part, by a negative feedback mechanism transduced through IκB-α, the major cytosolic inhibitor of NF-κB.

Key words: cytokine, inhibitory κB-α, α-melanocyte-stimulating hormone, pathophysiology, prostaglandin.

INTRODUCTION

α-Melanocyte-stimulating hormone (α-MSH) is a tridecaneuropeptide with potent anti-inflammatory activity [1]. α-MSH reduces fever, acute inflammation caused by local mediators such as cytokines, delayed hypersensitivity, and chronic and local inflammation [2]. The mechanism by which α-MSH exhibits immunomodulatory activities is not fully understood, but it is believed that α-MSH and related peptides have the potential to down-regulate pro-inflammatory cytokines such as interleukin (IL)-1 and tumour necrosis factor α, and to up-regulate an anti-inflammatory response through other cytokines such as IL-10 [3–5]. Recent evidence suggests that this pathway might be mediated by inhibition of the redox-sensitive nuclear factor κB (NF-κB), a transcription factor essential to the expression of pro-inflammatory genes encoding cytokines [6–9].

The translocation and activation of NF-κB in response to various stimuli are organized sequentially at the molecular level. In its inactive state, the heterodimeric NF-κB, which is composed mainly of two subunits, p65 (RelA) and p50 (NF-κB_1), is present in the cytoplasm associated with its inhibitory protein, inhibitory κB (IκB) [10]. On stimulation, for instance with cytokines, IκB-α undergoes phosphorylation, ubiquitination and proteolytic degradation, thereby unmasking the nuclear localization signal on p65 and permitting the nuclear translocation of the complex. One of the major mechanisms proposed for the α-MSH-mediated inhibition of NF-κB involves the suppression of reactive oxygen species (ROS) and reactive nitrogen species, thought to be transducing messengers for its activation [1–3,11]. In addition, it has been suggested that cytokines induce NF-κB activation by increasing intracellular ROS and reactive nitrogen species [12,13]. It is therefore likely that α-MSH down-regulates the cytokine-

Abbreviations used: EMSA, electrophoretic mobility-shift assay; IκB-α, inhibitory κB-α; IL, interleukin; IL-1ra, IL-1 receptor antagonist; LPS, lipopolysaccharide; KDPV, lysine-D-proline-valine; α-MSH, α-melanocyte-stimulating hormone; NF-κB, nuclear factor κB; NSAID, non-steroidal anti-inflammatory drug; PGE_2, prostaglandin E_2; rhIL-1, recombinant human interleukin 1; ROS, reactive oxygen species.

[1] To whom correspondence should be addressed (e-mail j.j.haddad@dundee.ac.uk).

dependent activation of NF-κB by counteracting the ROS-mediated induction of IκB kinases and the subsequent phosphorylations, thus retaining NF-κB in its cytosolic coupled form [14]. Furthermore, it has been reported that α-MSH blocks NF-κB activation through a cAMP-dependent pathway by activating β-adrenergic receptors [7,9].

The C-terminal tripeptide of α-MSH, lysine^{11}-D-proline-valine^{13} (KdPV), is anti-pyretic against leucocyte pyrogen [15], of which IL-1 is a major component [16], and is reported to have an anti-inflammatory activity [17]. Additionally, the hyperalgesic (nociceptive) potential of IL-1 and prostaglandin E_2 (PGE_2) is inhibited by KdPV, a tripeptide analogue of IL-1β (lysine^{193}-D-proline-valine^{195}) [18]. KdPV has also been shown to antagonize inflammatory responses mediated by IL-1β and PGE_2 [18,19]. It has yet to be ascertained whether or not the anti-inflammatory properties assigned to KdPV are due to its ability to down-regulate the translocation and activation of NF-κB in the alveolar epithelium. The aim of the present study was therefore to determine the mechanism of action of KdPV. We show in particular that KdPV inhibits lipopolysaccharide (LPS)-induced NF-κB translocation and activation and that the IL-1 receptor antagonism is involved in this mechanism. In addition, KdPV and IL-1 receptor antagonist (IL-1ra) decrease, in a dose-dependent manner, the LPS-mediated degradation of IκB-α, the major cytosolic inhibitor of NF-κB. We also show that KdPV and IL-1ra dose-dependently reverse the IL-1-induced activation of NF-κB and that blockage of the prostaglandin-forming cyclo-oxygenase cascade by the non-steroidal anti-inflammatory drug (NSAID) indomethacin attenuates LPS-induced NF-κB activation. These results indicate the involvement of prostanoid-sensitive and IL-1-sensitive mechanisms mediating LPS-induced NF-κB translocation/activation, a pathway involving negative feedback regulation by IκB-α.

MATERIALS AND METHODS

Chemicals and reagents

Unless indicated otherwise, chemicals of the highest analytical grade were purchased from Sigma–Aldrich. All experimental procedures involving the use of live animals were reviewed and approved under the Animals Act (1986) legislation (U.K.). α-Melanocyte-related tripeptide, KdPV, is synthesized from the C-terminus of α-MSH at residues 11–13 [18]. KdPV was custom-synthesized by Cambridge Research Biochemicals (Cambridge, U.K.), characterized by fast-atom-bombardment MS, amino acid analysis and analytical reverse-phase HPLC, and purified to at least 95% purity by preparative HPLC [National Institute for Biological Standards and Control (NIBSC), Potters Bar, Herts., U.K.]. This peptide is analogous to the amino acid sequence of IL-1$\beta^{193–195}$, thus serving as a non-selective antagonist of IL-1 receptor [18]. KdPV, which has been shown to antagonize and inhibit the effects of PGE_2 (ED_{50} 2.4 μmol/kg) and IL-1β (ED_{50} 0.76 μmol/kg) *in vivo* [18,19], was generously provided by Dr Stephen Poole (NIBSC), who first identified and isolated this and other tripeptides related to α-MSH. The cytokine recombinant human interleukin 1 (rhIL-1) was purchased from NIBSC; the freeze-dried powder was dissolved in physiological sterile saline and stored in aliquots at -20 °C. The specificity, purity and biological activity of rhIL-1 were determined and authenticated by NIBSC.

Epithelial primary cell cultures

Foetal alveolar type II epithelial cells were isolated from the lungs of foetuses of pregnant Sprague–Dawley rats, essentially as reported elsewhere [20,21]. In brief, foetal rats were removed by caesarean section at day 19 of gestation (term is 22 days); the lungs were excised, teased free from heart and upper airway tissue and finely minced, then washed free of erythrocytes with sterile, chilled Mg^{2+}- and Ca^{2+}-free Hanks balanced salt solution (HBSS) (0.5 ml per foetus). The cleaned lung tissue from each foetus was resuspended in 1 ml of HBSS containing trypsin (0.1 mg/ml), collagenase (0.06 mg/ml) and DNase I (0.012%, w/v) and was agitated at 37 °C for 20 min. The solution was then centrifuged at 100 ***g*** for 2 min to remove undispersed tissue; the supernatant was decanted into a sterile tube and an equal volume of DMEM (Dulbecco's modified Eagle's medium) with 10% (v/v) FCS (foetal calf serum) was added to the supernatant. After the supernatant had been passed through a sterile mesh (120 μm pore size), the filtrate was centrifuged at 420 ***g*** for 5 min, the pellet was resuspended in 20 ml of DMEM/FCS and the cells were placed into a T-150 culture flask for 1 h at 37 °C to enable fibroblasts and non-epithelial cells to adhere. Unattached cells were washed three times by centrifugation at 420 ***g*** for 5 min each and then seeded on 24 mm diameter Transwell-clear permeable supports (0.4 μm pore size; Costar) at a density of 5×10^6 cells per filter and were left to adhere overnight at 152 Torr (approx. 20.3 kPa; approx. 21% O_2) at 37 °C. DMEM/FCS was exchanged for 4 ml of pre-equilibrated serum-free PC-1 medium (Biowhittaker, Walkersville, MD, U.S.A.) 24 h later; cells were maintained in this medium until the experiment. The adenylate energy charge, an index of cell viability and competence, remained 0.7 or higher and transepithelial monolayer resistance was monitored constantly at 250–350 Ω cm^2 or more [20].

Determination of LPS-induced NF-κB translocation and activation

LPS treatment, Western blot analysis and electrophoretic mobility-shift assay (EMSA)

For the dose–response curve, cells were exposed for 24 h to LPS (0–10000 ng/ml) from *Escherichia coli* serotype 026:B6. After treatment, subcellular extracts were prepared essentially as described previously [20,21]. In brief, filters were washed twice in 5 ml of ice-cold pre-equilibrated PBS; cells [$(1–2) \times 10^7$] were collected and centrifuged at 420 ***g*** for 5 min at 4 °C. Nuclei were released by resuspending the pellet in 250 μl of buffer A containing (in mM): 10 Tris/HCl, pH 7.8, 10 KCl, 2.5 NaH_2PO_4, 1.5 $MgCl_2$, 1 Na_3VO_4, 0.5 dithiothreitol, 0.4 4-(2-aminoethyl)-benzenesulphonyl fluoride/HCl ('AEBSF'), and 2 μg/ml leupeptin, 2 μg/ml pepstatin A and 2 μg/ml aprotinin. The suspension was left in ice for 10 min followed by homogenization for 45 s at a moderate speed. Nuclei were collected by centrifuging the slurry at 4500 ***g*** for 5 min at 4 °C and were resuspended in 100 μl of buffer B [buffer A adjusted to (in mM): 20 Tris/HCl, pH 7.8, 420 KCl and 20% (v/v) glycerol]. The supernatant formed is termed the cytosolic extract. The nuclei were then lysed at 4 °C for 30 min with gentle agitation, the debris was cleared by centrifugation at 10000 ***g*** for a further 30 min at 4 °C and the supernatant was frozen in liquid nitrogen and stored at -70 °C until used. In all cases, protein contents were determined by the Bradford method with BSA as a standard. Cytosolic and nuclear proteins (20–25 μg) were resolved by SDS/PAGE [7.5% (w/v) gel] at room temperature and blotted to nitrocellulose membrane; non-specific binding sites were subsequently blocked. Mouse monoclonal IgG_1 anti-(IκB-α) (H-4), IgG_{2b} anti-(phosphorylated IκB-α) (B-9), rabbit polyclonal IgG anti-p50 (NLS), anti-p52 (K-27), anti-p65 (RelA; A), anti-p68 (RelB; C-19) and anti-p75 (c-Rel; N) (Santa Cruz Biotechnology) antibodies were used for primary detection. Anti-rabbit Ig-biotinylated antibody (Amersham Life Science) was employed for secondary detection

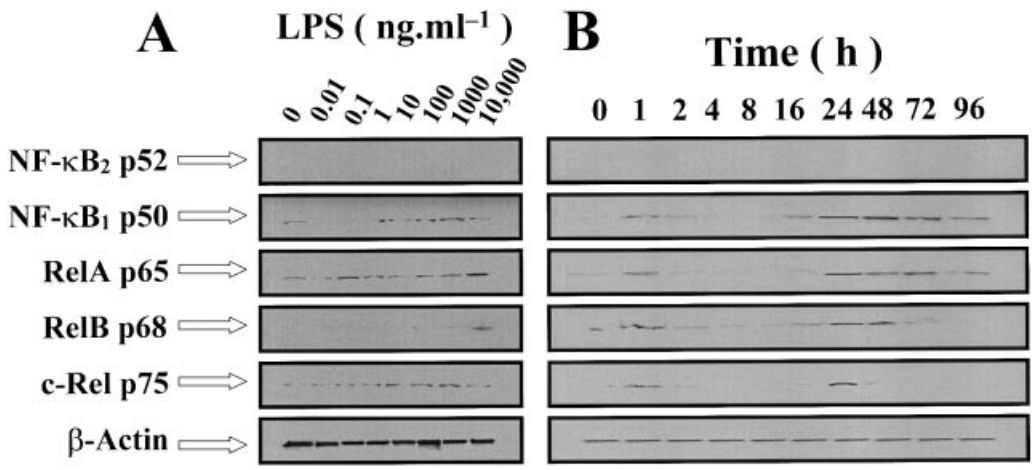

Figure 1 Effect of LPS on the nuclear composition of NF-κB subunits

(**A**) Western immunoblotting showing the dose-dependent (0–10000 ng/ml) variation in the abundance of the composition of NF-κB subunits in the nuclear compartment. (**B**) The time response to the administration of LPS (1000 ng/ml), showing the biphasic variations in NF-κB subunits, with rapid induction as early as 1 h after LPS administration and a late peak at 24–48 h. The housekeeping protein β-actin was used as an internal reference for semi-quantitative loading in parallel lanes. $n = 4$ independent experiments.

followed by the addition of streptavidin–horseradish-peroxidase conjugate and detected on film by chemiluminescence. β-Actin standard was used as an internal reference for semiquantitative loading in parallel lanes for each variable. Western blots were scanned by NIH MagiScanII and subsequently quantified with a UN-Scan-IT automated digitizing system (version 5.1; 32-bit), and the ratio of the density of the band to that of β-actin was subsequently measured. Nuclear extracts were analysed for DNA-binding activity of NF-κB by EMSA; supershift experiments with specific antibodies were performed as described previously [20,21]. Specific quantification of the corresponding DNA gel-shift bands was performed by phosphorimaging.

KDPV pretreatment and NF-κB translocation/activation

To the best of our knowledge, the role of KDPV as a modulator of signalling transduction mechanisms governing NF-κB translocation and activation is not known, either in the alveolar epithelium or in other tissues. To test the concept that KDPV intervenes in pathways mediated by NF-κB in the alveolar epithelium, cells were pretreated with KDPV (0–10 μg/ml) for 2 h and challenged with LPS (1 μg/ml) for 24 h, followed by assessment of NF-κB translocation and activation. This paper would therefore be the first to identify at the molecular level the biochemical role of KDPV in regulating NF-κB transduction pathways.

Pretreatment with IL-1ra and translocation/activation of NF-κB

IL-1ra blocks IL-1 receptors, thereby inhibiting the binding of IL-1; any subsequent secondary effects mediated by this cytokine are therefore obliterated [22]. Accordingly, cells were pretreated with IL-1ra (0–10 ng/ml) (NIBSC) for 2 h before exposure to LPS (1 μg/ml) for 24 h, followed by assessment of NF-κB translocation and activation.

Exogenous rhIL-1 and activation of NF-κB

Monolayers were exposed to increasing concentrations of rhIL-1 (0–30 ng/ml) and nuclear extracts were subsequently prepared as recounted previously. For pretreatments, cells were incubated in the presence of KDPV (0–10 μg/ml) or IL-1ra (0–10 ng/ml) for 2 h, washed twice in pre-equilibrated PC-1 medium and exposed to rhIL-1 (10 ng/ml) for 24 h. Nuclear extracts were subsequently prepared for analysis of the DNA binding activity.

Indomethacin and the activation of NF-κB

Epithelial cells were independently pretreated with indomethacin (0–10 μg/ml), an inhibitor of the prostaglandin-forming cyclo-oxygenase [23], for 2 h, before exposure to LPS (1000 ng/ml) for 24 h. Nuclei were subsequently prepared and nuclear extracts were used to study the DNA binding activity by EMSA.

Assessment of endogenous IL-1β biosynthesis in response to LPS by using ELISA

Cells were grown as above at a density of 5×10^6 cells per filter and exposed to LPS (1000 ng/ml) the next day. Aliquots of the supernatant were withdrawn at specific intervals (0–96 h) as indicated, then centrifuged (3000 ***g***) to remove residual debris. IL-1β in cell-free supernatants was measured by sandwich ELISA. Immunoaffinity-purified polyclonal rabbit anti-rat IL-1β (1 μg/ml) antibody was used to coat high-binding microtitre plates (MaxiSorp; Nunc) in bicarbonate buffer [0.1 M $NaHCO_3$/0.1 M NaCl (pH 8.2)], essentially as detailed elsewhere [22]. After blocking in 3% (w/v) BSA, recombinant (standard) and biotinylated (recognition) immunoaffinity-purified sheep anti-rat IL-1β antibody (a gift from Dr Stephen Poole, NIBSC) were employed for secondary detection. The colour was developed with streptavidin-poly-(horseradish peroxidase) (Amersham, Little Chalfont, Bucks., U.K.) coupled with the chromagen 3,3′,5,5′-tetramethylbenzidine (TMB) in the presence of 1 mM H_2O_2. A_{450} was read; inter-assay and intra-assay coefficients of variation were less than 10%.

Statistical analysis and data handling

Experimental results are expressed as means ± S.E.M. for at least three independent cell cultures. Statistical analysis was performed

by one-way analysis of variance, followed by Tukey's post hoc test to determine the significance of mean separation between treatments. The a priori level of significance at 95% confidence was considered to be $P < 0.05$.

RESULTS

LPS-induced NF-κB nuclear translocation, activation and specificity of the NF-κB–DNA complex

A Western immunoelectroblotting analysis of NF-κB subunit composition in response to challenge with LPS is shown in Figure 1(A). The abundance of NF-κB_2 (p52) was not affected and that of p68 was marginally induced in the nuclear compartment, whereas those of NF-κB_1 (p50), RelA (p65) and c-Rel (p75) increased with ascending LPS concentration in a dose-dependent manner. The most prominent effect of LPS was observed with p65, the major transactivating member of NF-κB/Rel family (Figure 1A). The time–response gels showing the biphasic variation (early and late translocation) in NF-κB subunit composition are shown in Figure 1(B). This biphasic effect of LPS on NF-κB subunit composition shows an early translocation event at 1 h (for p50, p65, p68 and p75), thereafter subsiding to re-elevate at a later stage at 16 h (for p50 and p68) and 24 h (for p50, p65, p68 and p75), reaching an apparent peak between 24–48 h, declining afterwards (Figure 1B).

In parallel with selective NF-κB nuclear translocation, LPS induced a dose-dependent activation of NF-κB DNA binding activity, as shown in Figure 2(A). LPS caused a marginal increase in NF-κB activity at concentrations of 100 ng/ml and above. A concentration of 1000 ng/ml induced maximum induction (Figure 2A), an effect that was sustained at the highest dose used (10000 ng/ml). The histogram analysis of the gel-shift bands quantified by UniScan phosphorimaging determined as percentages of maximal activation relative to control (0 ng/ml LPS) is shown in Figure 2(B). A supershift analysis indicating the major composition of the NF-κB complex (p50–p65) is shown in Figure 2(C). Consecutively arranged, lane 1 is included as a negative control (no LPS), lane 2 as a positive control (LPS alone; 1000 ng/ml), and lanes 3–7 as the variables including LPS in the presence of selective antibodies raised against NF-κB subunits (Figure 2C).

To confirm the specificity determination of the complexed bands obtained for NF-κB, we added a mutant oligonucleotide (3 bp mis-sense control, 5′-AGTTGA**AAA**GACTTTCCCAG-GC-3′; mutant sequence underlined) and a 50-fold or 100-fold excess of unlabelled oligonucleotide competitor, both of which completely abolished the binding of NF-κB (Figure 2D). The control lane contained no nuclear extract.

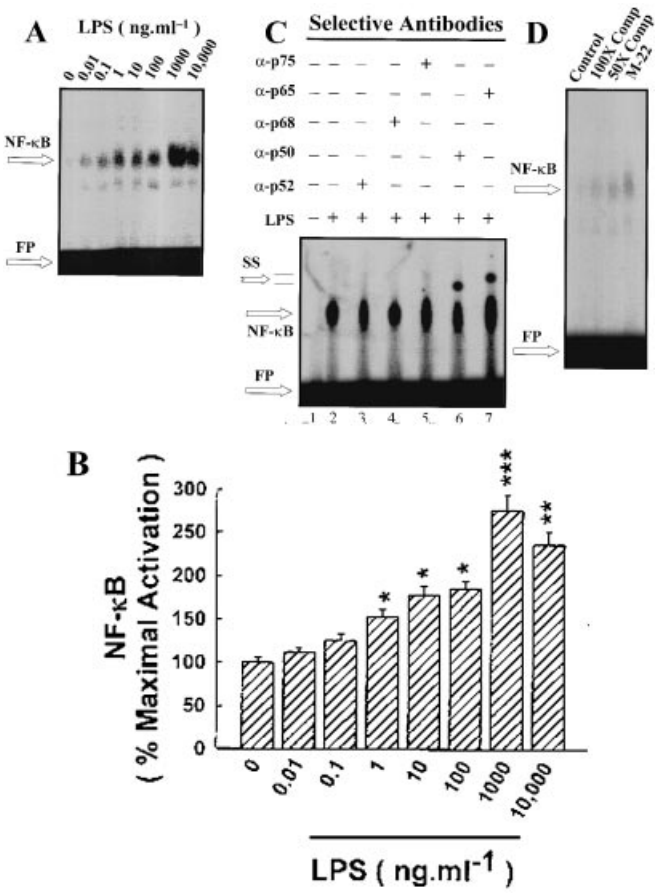

Figure 2 LPS-mediated NF-κB activation and heterodimer complex

(**A**) A representative EMSA exhibiting the activation of NF-κB with increasing LPS concentration. The maximum activity is observed with an LPS concentration of 1000 ng/ml, the optimum dose used subsequently. (**B**) Histogram analysis of LPS-induced NF-κB activation, as determined by quantifying the shifted bands by UniScan phosphorimaging plotted as the percentage of maximal activation relative to the band obtained with the control (0; no LPS) $^{*}P < 0.05$, $^{**}P < 0.01$, $^{***}P < 0.001$, compared with control. (**C**) Supershift analysis by selective antibodies raised against NF-κB subunits, revealing the presence of a p50–p65 heterodimer within the nucleus. Lane 1, no nuclear extracts; lane 2, positive control of LPS (1000 ng/ml)-treated cells; lanes 3–7, nuclear extracts of LPS-treated cells in the presence of specific antibodies against NF-κB subunits, as indicated. (**D**) Specificity of the NF-κB–DNA complex as determined by unlabelled competition and mutation. FP, free probe (lower open arrows); upper open arrows, NF-κB–DNA complex (in this and subsequent figures); SS, position of the supershift. $n = 4$ independent experiments.

LPS-mediated degradation and phosphorylation of IκB-α

Cell treatment with LPS induced a dose-dependent degradation of IκB-α in the cytosolic compartment, with no apparent changes within the nucleus (Figure 3A). The histogram analysis of the corresponding bands determined relative to β-actin, a housekeeping gene product, is given in Figure 3(B), showing a pseudo-Voigt regression analysis with ascending concentrations of LPS. The time–response gels showing variations in IκB-α abundance and its phosphorylated form in the cytoplasm with LPS (1000 ng/ml) are given in Figure 3(C). LPS-induced degradation of IκB-α became significantly different from control (no LPS) at 4 h, where its abundance sharply declined up to 96 h. In contrast, the abundance of the phosphorylated form of IκB-α increased exponentially beginning 4 h after the addition of LPS (1000 ng/ml) and maximizing at 48–96 h (Figure 3C). The histogram analysis of the corresponding bands of IκB-α and its phosphorylated form relative to β-actin with pseudo-Voigt regression analysis is shown in Figure 3(D). This observation indicates that, after LPS stimulation, IκB is phosphorylated, ubiquitinated and degraded (ubiquitin–proteasome mediated), thereby unmasking the localization signal sequence for NF-κB translocation and activation.

KDPV-dependent inhibition of LPS-induced nuclear translocation and activation of NF-κB

Because LPS induced a dose- and time-dependent nuclear accumulation of p50, p65 and p75, we next determined whether KDPV was mitigating or attenuating this selective response. As shown in Figure 4(A), KDPV decreased, in a dose-dependent manner, the nuclear abundance of p50, at doses of 0.1 μg/ml or

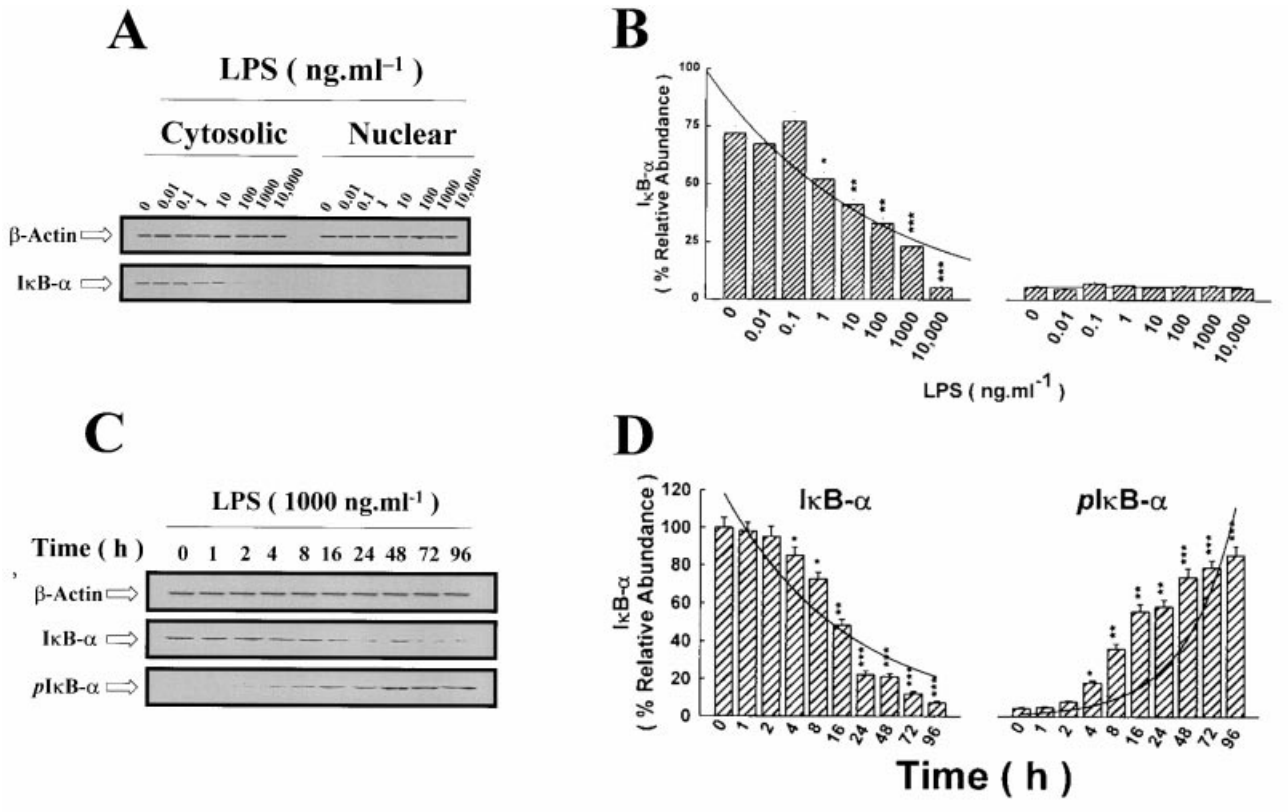

Figure 3 Effect of LPS on IκB-α phosphorylation and degradation

(**A**) Western analysis of LPS-induced degradation of IκB-α, showing the dose-dependent effect in the cytosolic, but not in the nuclear, compartment. (**B**) Histogram analysis of IκB-α degradation. $^{*}P < 0.05$, $^{**}P < 0.01$, $^{***}P < 0.001$, compared with control. (**C**) LPS (1000 ng/ml) mediates the inhibitory degradation of IκB-α and up-regulates its phosphorylation in the cytosolic compartment in a time-dependent manner, an effect starting at 4 h and continuing thereafter. The housekeeping protein β-actin was used as an internal reference for semi-quantitative loading in parallel lanes. Abbreviation: *p*IκB-α, phosphorylated form of IκB-α. (**D**) Histogram analysis of IκB-α degradation and phosphorylation. $^{*}P < 0.05$, $^{**}P < 0.01$, $^{***}P < 0.001$, compared with control (0 h). $n = 4$ independent experiments.

more. The nuclear abundance of p65 and p75 was decreased by KDPV at doses of 1 μg/ml or more (Figure 4A). The histogram analysis of the intensity of the corresponding bands relative to β-actin is given in Figure 4(B). KDPV exhibited a dose-dependent inhibition of NF-κB DNA binding activity (Figure 4C), with maximum inhibition at 10 μg/ml. The histogram analysis of the corresponding bands of NF-κB complex is shown in Figure 4(D).

IL-1ra-dependent inhibition of LPS-induced nuclear translocation and activation of NF-κB

A prominent, dose-dependent, decrease in LPS-induced nuclear accumulation of p50, p65 and p75 is observed with pretreatment with IL-1ra (Figure 5A), at doses of 0.1 ng/ml or more. The histogram analysis of the intensity of the corresponding bands relative to β-actin is given in Figure 5(B). In a manner similar to the effect of KDPV, IL-1ra showed a dose-dependent inhibition of LPS-induced NF-κB activation (Figure 5C), with maximum inhibition at 10 ng/ml. The histogram analysis of the corresponding bands of NF-κB complex is shown in Figure 5(D).

Effect of KDPV and IL-1ra on LPS-mediated degradation and phosphorylation of IκB-α

LPS induced a dose-dependent degradation of IκB-α in the cytosolic compartment, an effect that was substantially reversed, in a dose-dependent manner, by KDPV and IL-1ra at 24 h (Figure 6A). As shown in Figure 6(B), KDPV reversed IκB-α degradation, an observation significantly different from the control (LPS alone) at doses of 0.1 μg/ml or more. Similarly, IL-1ra reversed IκB-α degradation in a dose-dependent manner at doses of 1 ng/ml or more. This reversal effect of KDPV and IL-1ra was accompanied by a dose-dependent inhibition of IκB-α phosphorylation at doses of 1 μg/ml or more (KDPV) and 0.1 ng/ml or more (IL-1ra) (Figure 6B). An analysis of the IC_{50} and EC_{50} values of KDPV and IL-1ra on LPS-mediated NF-κB translocation/activation and IκB-α abundance is given in Table 1. IC_{50} and EC_{50} were extrapolated from the negative and positive slopes respectively of the linear regression curves.

Role of KDPV and IL-1ra in the IL-1-mediated activation of NF-κB

The time–response curve showing the variation in IL-1β concentration with LPS (1 μg/ml) is shown in Figure 7(A). The concentration of IL-1β began to increase at 1–2 h, with an early peak at 2–4 h and declining thereafter, but was significantly persistent up to 24 h, followed by a depression plateau beyond 48 h (Figure 7A). The dose-dependent activation of NF-κB by exogenous rhIL-1 (24 h) is shown in Figure 7(B), revealing a maximum induction at 10 ng/ml, the dose that we used subsequently to investigate the potential inhibitory roles of KDPV and

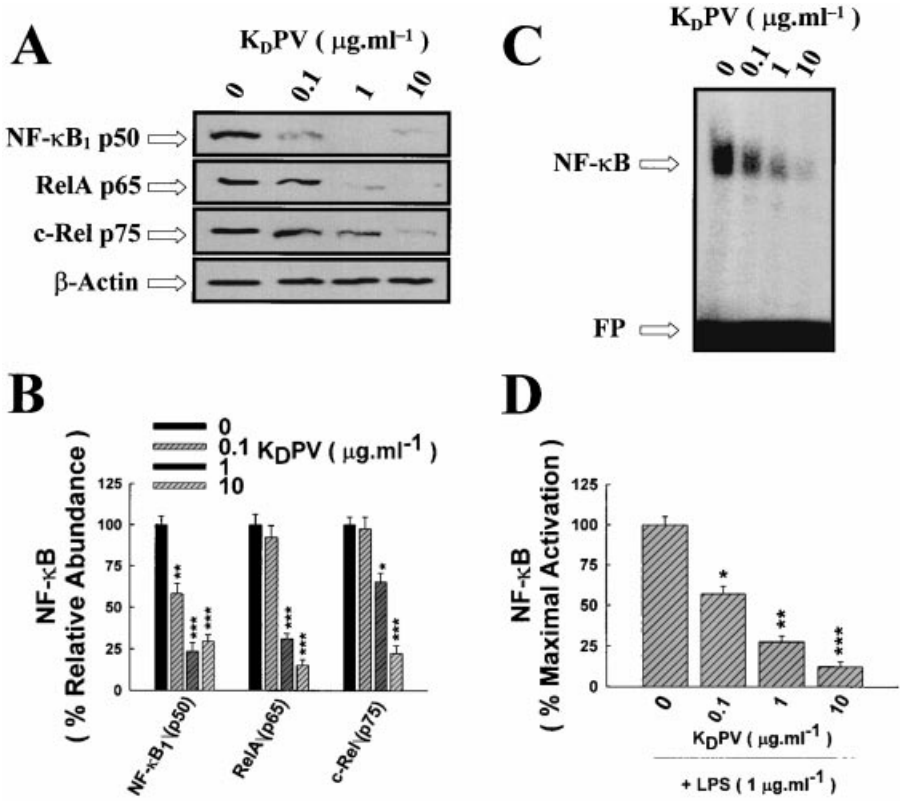

Figure 4 Role of KDPV in LPS-induced NF-κB nuclear translocation and activation

(**A**) Analysis of KDPV-induced inhibition of LPS-dependent nuclear localization of p50, p65 and p75, revealing a dose-dependent reversal of the effect of LPS (1000 ng/ml) at 24 h. (**B**) Histogram analysis of NF-κB nuclear composition in response to KDPV. $^{*}P < 0.05$, $^{**}P < 0.01$, $^{***}P < 0.001$, compared with control. The housekeeping protein β-actin was used as an internal reference for semi-quantitative loading in parallel lanes. $n = 4$ independent experiments. (**C**) DNA binding activity of NF-κB complex in response to pretreatment with KDPV for 2 h, showing the dose-dependent inhibition of LPS-induced activation. (**D**) Histogram analysis of the gel-shifted bands, revealing KDPV-induced NF-κB inhibition. $^{*}P < 0.05$, $^{**}P < 0.01$, $^{***}P < 0.001$, compared with control. $n = 4$ independent experiments.

IL-1ra on IL-1-mediated activation of NF-κB. Interestingly, both KDPV and IL-1ra abrogated, in a dose-dependent manner, the IL-1-induced activation of NF-κB (Figure 7C).

Role of NSAIDs in the LPS-induced activation of NF-κB

Pretreatment with indomethacin, an NSAID drug that inhibits the prostaglandin-forming cyclo-oxygenase cascade [23], substantially suppressed LPS-dependent activation of NF-κB at doses of 1 μg/ml or more (Figure 8A). The histogram analysis of the corresponding gel-shift NF-κB–DNA bands is shown in Figure 8(B).

DISCUSSION

The present study shows that the α-MSH-related tripeptide KDPV, an analogue of IL-1$\beta^{193–195}$ [18], exhibits an anti-inflammatory role by interfering negatively with the transduction pathway regulating the translocation and activation of NF-κB [10]. This tripeptide has been shown to down-regulate inflammation by suppressing and antagonizing the effects of IL-1β and PGE_2 [18,19]. However, the underlying mechanism of transduction in the foetal alveolar epithelium of the developing lung remains to be elucidated.

Although the inflammatory signals mediated by LPS are recognized in other systems and cell models, this role in the foetal alveolar epithelium is not well characterized. The administration of LPS regulated differentially, in a dose-dependent manner, NF-κB nuclear subunit translocation *in vitro*. Despite the observation that LPS has no influence on the unit composition of $NF\text{-}\kappa B_2$ (p52) and a mild effect on RelB (p68), its stimulatory effect on $NF\text{-}\kappa B_1$ (p50), c-Rel (p75) and RelA (p65), the major transactivating member of the Rel family [10,24], is evidently prominent. There is a dose-dependent induction of the nuclear accumulation of p50, p65 and p75, suggesting specific up-regulation. The observation that LPS-induced NF-κB nuclear accumulation is biphasic remains of particular interest. We have previously shown that NF-κB activation in the alveolar epithelium in response to an ascending Δp_{O_2} regimen (oxyexcitation) followed a biphasic pattern (early peak at 5–15 min and a late peak at 24–48 h) [25], consistent with the accumulation of selective subunits within the nuclear compartment (J. J. E. Haddad, R. E. Olver and S. C. Land, unpublished work). Although the molecular basis of this biphasic behaviour is unclear, we can speculate that the induction of an NF-κB-mediated pathway within the alveolar space occurs almost promptly after the implementation of a given stimulus (such as Δp_{O_2} and LPS), thereafter taken over by other secondary mediators (such as ROS and cytokines), which when accumulating within intracellular compartments have the potential to trigger another boost of NF-κB via a positive feedback loop. Furthermore, the release of free NF-κB upon extracellular

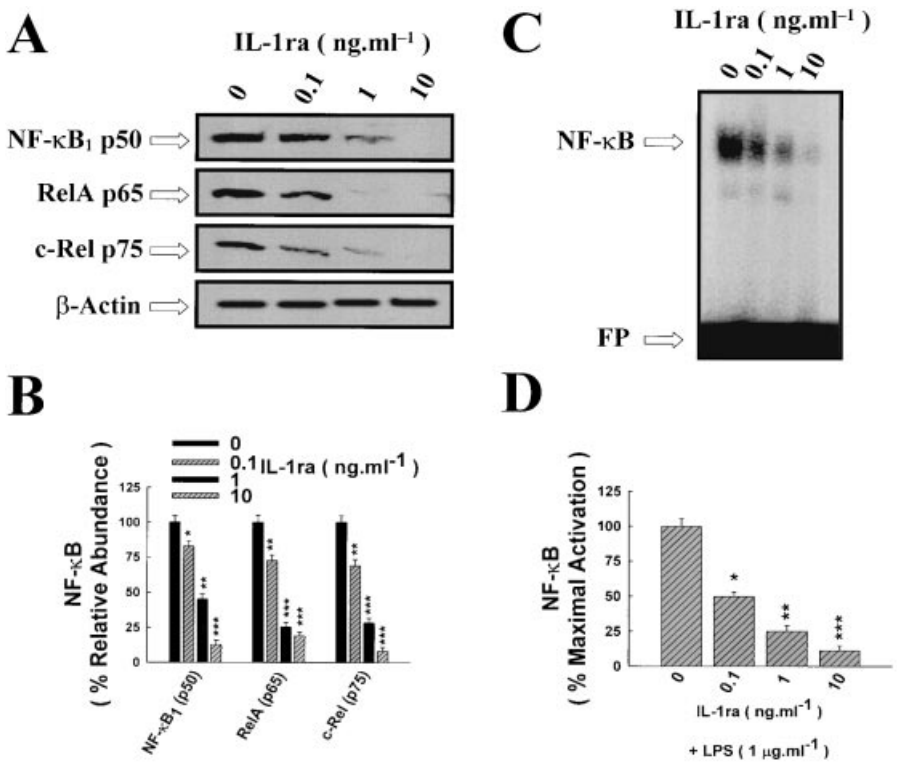

Figure 5 Role of IL-1ra in LPS-induced NF-κB nuclear translocation and activation

(**A**) Analysis of IL-1ra-induced inhibition of LPS-dependent nuclear localization of p50, p65 and p75, revealing a dose-dependent reversal of the effect of LPS at 24 h. (**B**) Histogram analysis of NF-κB nuclear composition in response to IL-1ra. $^{*}P < 0.05$, $^{**}P < 0.01$, $^{***}P < 0.001$, compared with control. The housekeeping protein β-actin was used as an internal reference for semi-quantitative loading in parallel lanes. (**C**) DNA binding activity of NF-κB complex in response to pretreatment with IL-1ra for 2 h, showing the dose-dependent inhibition of LPS-induced activation. (**D**) Histogram analysis of IL-1ra-induced NF-κB inhibition. $^{*}P < 0.05$, $^{**}P < 0.01$, $^{***}P < 0.001$, compared with control. $n = 4$ independent experiments. FP, free probe.

stimulation, which is due to IκB phosphorylation and degradation, leads to DNA binding to initiate transcription of related genes, including immunoreceptors, cytokines and, interestingly, its own inhibitor, IκB [10,24]. Two unique features of the NF-κB–IκB complex system are deduced from its feedback regulation. The transcriptional activation of NF-κB triggers the synthesis of IκB; NF-κB activated transcription is maintained by the continuous degradation of IκB, which is sustained by an extracellular stimulus [26]. Thus the expression of IκB parallels both NF-κB activity and the duration of the activating extracellular stimulation, suggesting that this temporal parallelism between IκB accumulation/degradation and an effective external stimulation is a mechanism allowing dual, biphasic, regulation of NF-κB within the alveolar space.

The selective accumulation of NF-κB subunits in the nuclear compartment prompted us to investigate whether LPS is inducing a parallel DNA binding activity. It is evident that there is a dose-dependent activation of NF-κB, where the p50–p65 complex is recognized as the major Rel dimer involved in the transduction pathway. This extends our previous reports in which we showed a particular involvement of p65 in transducing mechanisms mediating the regulatory potential of NF-κB in the perinatal epithelium and at different stages of gestational lung development [20,21,27]. Of particular interest is the observation that LPS-dependent translocation and activation of NF-κB are mediated through an IκB-α-dependent pathway. LPS induced IκB-α degradation in a dose-dependent manner, an effect accompanied by inducing its phosphorylation, thereby allowing its degradation by the proteasome system and subsequently permitting the nuclear translocation and activation of the NF-κB complex [14,28].

The C-terminal tripeptide of α-MSH, Lys^{11}-D-$Pro\text{-}Val^{13}$ (KdPV), is antipyretic against leucocyte pyrogen, of which IL-1 is a major component [15,16]. In addition it is reported to have an anti-inflammatory activity [17] and acts as a potent analgesic analogue *in vivo* [18,19]. We have shown previously that KdPV reversed LPS-induced hyperalgesia *in vivo* [22], an effect mimicked by IL-1ra as determined by pain-related behaviour. KdPV was first identified by Poole et al. [18] as an α-MSH-related tripeptide analogue to the sequence of IL-1$\beta^{193–195}$, thus possessing peripheral analgesic activities mediated by the κ-opioid receptors [18]. Subsequently it was recognized as a potent, irreversible antagonist of the hyperalgesic and inflammatory effects of PGE_2 and IL-1 [18,19]. α-MSH and related peptides have been shown previously to modulate the production of reactive oxygen and nitrogen species [2,3,29], to regulate the release of pro-inflammatory mediators such as tumour necrosis factor α [30] and IL-6 [31], and to induce the release of cyclic nucleotides (cAMP and cGMP) [2]. Furthermore, it has been reported that α-MSH protects against renal injury after ischaemia [32] and reduces LPS-induced liver inflammation *in vivo* [33]. Of particular interest is accumulating evidence that suggests the intervention of α-MSH in signalling pathways mediating the suppression of the nuclear localization and activation of NF-κB, thought to have a

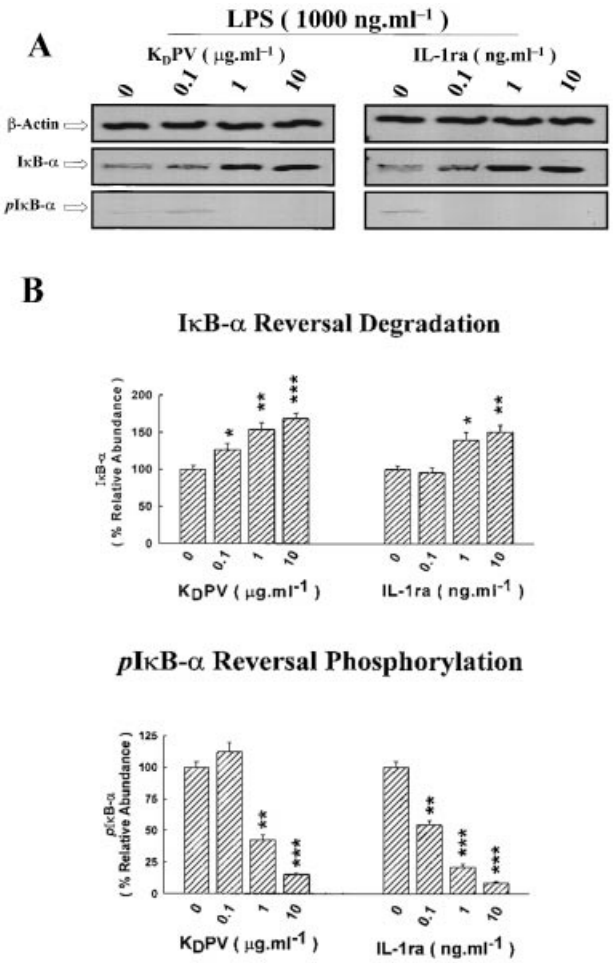

Figure 6 Effect of KDPV/IL-1ra on LPS-dependent IκB-α phosphorylation and degradation

(**A**) KDPV-dependent and IL-1ra-dependent reversal of the effect of LPS on IκB-α phosphorylation and degradation. KDPV and IL-1ra induced the up-regulation of IκB-α and suppressed its phosphorylation. The housekeeping protein β-actin was used as an internal reference for semi-quantitative loading in parallel lanes. Abbreviation: pIκB-α, phosphorylated form of IκB-α. (**B**) Histogram analysis of the dose–response results. $^{*}P < 0.05$, $^{**}P < 0.01$, $^{***}P < 0.001$, compared with control. $n = 4$ independent experiments.

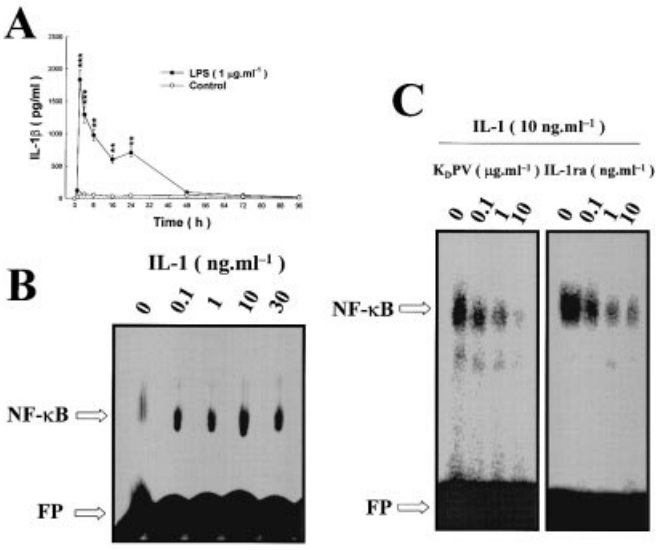

Figure 7 Role of exogenous rhIL-1 in NF-κB activation and the effect of KDPV/IL-1ra

(**A**) Time-dependent analysis of intracellular accumulation (biosynthesis) of IL-1β in response to LPS (1000 ng/ml). $^{**}P < 0.01$, $^{***}P < 0.001$, compared with control at the same time points. Symbols: ●, LPS; ○, control. (**B**) A representative EMSA at 24 h showing the dose-dependent effect of exogenous rhIL-1 on the activation of NF-κB. FP, free probe. (**C**) EMSAs revealing the dose-dependent effect of pretreatment with KDPV and IL-1ra for 2 h on NF-κB activation induced by rhIL-1 (10 ng/ml). FP, free probe.

major role in regulating the transcription of genes encoding cytokines [8,9,11,21,26,34]. However, the signalling mechanisms mediating the effect of this novel tripeptide in the foetal alveolar epithelium remain to be elucidated. These observations therefore prompted us to decipher the signalling pathways involved in mediating the effects of α-MSH-related tripeptide, KDPV. Here we show that KDPV exhibits an anti-inflammatory potential in the alveolar epithelium by regulating the nuclear localization and subsequent activation of NF-κB in an IκB-dependent mechanism.

KDPV selectively regulated the nuclear translocation of NF-κB subunits, with a prominent effect on p50, p75 and the major transactivating member of this family, RelA (p65). In addition, we report a dose-dependent inhibition of LPS-induced NF-κB activation, implicating a negative involvement for KDPV in signalling pathways mediating NF-κB translocation and activation. The ability of KDPV to antagonize the effects of both PGE_2 and IL-1 allows us to suggest that both prostanoids (PGE_2) and pro-inflammatory cytokines (IL-1β) are involved in the transduction pathways mediating NF-κB translocation/activation. This is supported by the evidence that indomethacin,

Table 1 Analysis of the IC_{50} and EC_{50} values of KDPV and IL-1ra on LPS-mediated NF-κB translocation/activation and IκB-α abundance in the alveolar epithelium

Results are means ± S.E.M.; $n = 4$ for each result. IC_{50} and EC_{50} values were extrapolated from the negative and positive slopes respectively of the linear regression curves.

	NF-κB subunits	IC_{50} (ng/ml)			EC_{50} (ng/ml)		
		LPS	KDPV	IL-1ra	LPS	KDPV	IL-1ra
NF-κB intensity	p50	–	3520 ± 120	4.25 ± 0.17	–	–	–
	p65	–	4230 ± 250	3.56 ± 0.14	–	–	–
	p75	–	5800 ± 320	2.97 ± 0.10	–	–	–
NF-κB activity		–	2640 ± 150	2.12 ± 0.13	1.02 ± 0.05	–	–
NF-κB-α inhibitor		697.2 ± 35.7	–	–	–	5480 ± 210	9.20 ± 0.25

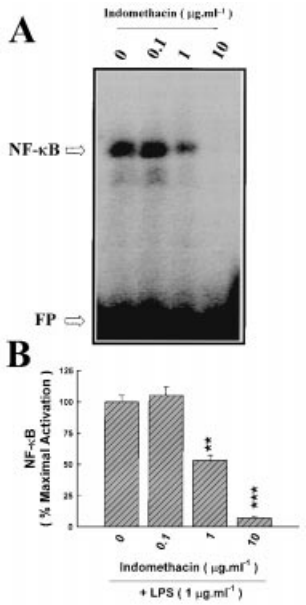

Figure 8 Role of NSAIDs in LPS-induced NF-κB activation

(**A**) A representative EMSA showing the attenuating effect of indomethacin on NF-κB activation (24 h) induced by 1 μg/ml LPS (present in all lanes). (**B**) Histogram analysis of the corresponding gel-shifted bands. $^{**}P < 0.01$, $^{***}P < 0.001$, compared with control. FP, free probe.

known to inhibit the prostaglandin-forming cyclo-oxygenases (COX-1 and COX-2) [23], abrogated the LPS-induced activation of NF-κB, suggesting that prostanoids, such as PGE_2, are involved, at least partly, in the transduction pathway mediating the effect of endotoxin on NF-κB. To confirm and support the involvement of an IL-1-dependent pathway, we tested the hypothesis that selective blockage of IL-1 receptors by IL-1ra would ameliorate the LPS-induced activation of NF-κB. In a manner similar to KDPV, IL-1ra inhibited the nuclear localization of selective Rel members, accompanied by a parallel depression of NF-κB activation, suggesting the involvement of IL-1 in NF-κB-mediated pathways. Taken together, these results provide evidence for the involvement of PGE_2-dependent (NSAID-sensitive) and IL-1-dependent (IL-1ra-sensitive) pathways mediating the translocation/activation of NF-κB in the alveolar epithelium.

The nuclear localization of NF-κB requires its dissociation from its cytosolic inhibitor, IκB-α [33]. This pathway is augmented by the phosphorylation of IκB-α on serine/threonine residues, a necessary step for the dissociation of NF-κB/IκB-α complexes, thereby unmasking the nuclear localization sequence on NF-κB and permitting the recognition of IκB-α by the ubiquitin–proteasome system for subsequent degradation. This sequential arrangement ultimately results in the release of NF-κB subunits from the inhibitor IκB-α, permitting translocation and the promotion of gene transcription. KDPV decreased LPS-dependent degradation of IκB-α in the cytosol, leading to its accumulation, an effect mimicked by IL-1ra. This effect was dependent on IκB-α phosphorylation; both KDPV and IL-1ra prevented the LPS-mediated phosphorylation of IκB-α. Therefore the KDPV- and IL-1ra-dependent inhibition of NF-κB localization and activation is mediated through IκB-α. This pathway implicates an organized sequential mechanism in mediating the effect of endotoxin on NF-κB.

The present study investigated a novel biochemical immunoregulatory potential of KDPV, IL-1ra and NSAIDs by exhibiting an inhibitory effect on NF-κB translocation and activation. In particular, we show the following: (1) LPS differentially, but selectively, up-regulated NF-κB subunit translocation/activation, an effect mediated through IκB-α phosphorylation and degradation; (2) KDPV selectively inhibited the translocation of NF-κB subunits and subsequently suppressed its activation, similarly to the inhibitory effects of IL-1ra; (3) KDPV and IL-1ra reversed the LPS-induced degradation of IκB-α, allowing its accumulation in the cytosol through suppression of its phosphorylation; (4) LPS induced a time-dependent accumulation of endogenous IL-1, and exogenous administration of rhIL-1 dose-dependently up-regulated NF-κB activation; this potential induction was abrogated by KDPV and IL-1ra; and (5) NSAID administration, which blocked the prostaglandin-forming cyclo-oxygenases, attenuated the LPS-dependent induction of NF-κB activation. These results indicate that the induction by LPS of NF-κB in the alveolar epithelium is mediated through an IκB-α-dependent mechanism and that the antagonism by KDPV and IL-1ra of NF-κB translocation/activation involves both prostanoid (NSAID-sensitive) and IL-1-dependent (KDPV- and IL-1ra-sensitive) pathways. The anti-inflammatory potential of KDPV tripeptide is therefore mediated through suppression of the NF-κB signalling transduction pathway in an IκB-dependent mechanism.

We thank Dr Stephen Poole (NIBSC, Potters Bar, Herts., U.K.) for providing ELISA reagents and the tripeptide KDPV (J.J.H.). J.J.H. is a recipient of the George John Livanos prize (London). This work was supported by the U.K. MRC, and by Anonymous Trust and Tenovus-Scotland grants (S.C.L.).

REFERENCES

1 Catania, A. and Lipton, J. M. (1993) Alpha-melanocyte stimulating hormone in the modulation of host reactions. Endocr. Rev. **14**, 564–576
2 Star, R. A., Rajora, N., Huang, J., Stock, R. C., Catania, A. and Lipton, J. M. (1995) Evidence of autocrine modulation of macrophage nitric oxide synthase by alpha-melanocyte-stimulating hormone. Proc. Natl. Acad. Sci. U.S.A. **92**, 8016–8020
3 Galimberti, D., Baron, P., Meda, L., Prat, E., Scarpini, E., Delgado, R., Catania, A., Lipton, J. M. and Scarlato, G. (1999) Alpha-MSH peptides inhibit production of nitric oxide and tumour necrosis factor-alpha by microglial cells activated with beta-amyloid and interferon gamma. Biochem. Biophys. Res. Commun. **263**, 251–256
4 Weiss, J. M., Sundar, S. K., Cierpial, M. A. and Ritchie, J. C. (1991) Effects of interleukin-1 infused into brain are antagonized by alpha-MSH in a dose-dependent manner. Eur. J. Pharmacol. **192**, 177–179
5 Bhardwaj, R. S., Shwarz, A., Becher, E., Mahanke, K., Aragane, Y., Shwarz, T. and Luger, T. A. (1996) Pro-opiomelanocortin-derived peptides induce IL-10 production in human monocytes. J. Immunol. **156**, 2517–2521
6 Ichiyama, T., Sakai, T., Catania, A., Barsh, G. S., Furukawa, S. and Lipton, J. M. (1999) Systemically administered α-melanocyte-stimulating peptides inhibit NF-κB activation in experimental brain inflammation. Brain Res. **836**, 31–37
7 Ichiyama, T., Sakai, T., Catania, A., Barsh, G. S., Furukawa, S. and Lipton, J. M. (1999) Inhibition of peripheral NF-κB activation by central action of α-melanocyte-stimulating hormone. J. Neuroimmunol. **99**, 211–217
8 Ichiyama, T., Zhao, H., Catania, A., Furukawa, S. and Lipton, J. M. (1999) α-Melanocyte-stimulating hormone inhibits NF-κB activation and IκB-α degradation in human glioma cells and in experimental brain inflammation. Exp. Neurol. **157**, 359–365
9 Manna, S. K. and Aggarwal1, B. B. (1998) Alpha-melanocyte-stimulating hormone inhibits the nuclear transcription factor NF-kappa B activation induced by various inflammatory agents. J. Immunol. **161**, 2873–2880
10 Siebenlist, U., Franzoso, G. and Brown, K. (1994) Structure, regulation and function of NF-κB. Annu. Rev. Cell Biol. **10**, 405–455
11 Schreck, R., Meier, B., Männel, D. N., Dröge, W. and Baeuerle, P. A. (1992) Dithiocarbamates as potent inhibitors of nuclear factor kappa B activation in intact cells. J. Exp. Med. **175**, 1181–1194
12 Saugstad, O. D. (1985) Oxygen radicals and pulmonary damage. Pediatrica Pulmonol. **1**, 167–175

13 Fu, K., Sarras Jr, M. P., De Lisle, R. C. and Andrews, G. K. (1997) Expression of oxidative stress-responsive genes and cytokine genes during caerulein-induced acute pancreatitis. Am. J. Physiol. **273**, G696–G705
14 Woronicz, J. D., Gao, X., Cao, Z., Rothe, M. and Goeddel, D. V. (1997) IκB kinase-β: NF-κB activation and complex formation with IκB kinase-α and NIK. Science **278**, 866–869
15 Richards, D. B. and Lipton, J. M. (1984) Effect of α-MSH 11–13 (lysine-proline-valine) on fever in the rabbit. Peptides **5**, 815–817
16 Dinarello, C. A. (1984) Interleukin-1. Rev. Infect. Dis. **6**, 51–95
17 Hiltz, M. E. and Lipton, J. M. (1990) Alpha-MSH peptides inhibit acute inflammation and contact sensitivity. Peptides **11**, 979–982
18 Poole, S., Bristow, A. F., Lorenzetti, B. B., Gaines Das, R. E., Smith, T. W. and Ferriera, S. H. (1992) Peripheral analgesic activities of peptides related to alpha-melanocyte stimulating hormone and interleukin-1$\beta^{193–195}$. Br. J. Pharmacol. **106**, 489–492
19 Ferreira, S. H., Lorenzetti, B. B., Bristow, A. F. and Poole, S. (1988) Interleukin-1β as a potent hyperalgesic agent antagonized by a tripeptide analogue. Nature (London) **334**, 698–700
20 Haddad, J. J. E. and Land, S. C. (2000) O_2-evoked regulation of HIF-1α and NF-κB in perinatal lung epithelium requires glutathione biosynthesis. Am. J. Physiol. Lung Cell. Mol. Physiol. **278**, L492–L503
21 Haddad, J. J. E., Olver, R. E. and Land, S. C. (2000) Antioxidant/pro-oxidant equilibrium regulates HIF-1α and NF-κB redox sensitivity. Evidence for inhibition by glutathione oxidation in alveolar epithelial cells. J. Biol. Chem. **275**, 21130–21139
22 Safieh-Garabedian, B., Kanaan, S. A., Haddad, J. J., Abou Jaoude, P., Jabbur, S. J. and Saadé, N. E. (1997) Involvement of interleukin-1β, nerve growth factor and prostaglandin E_2 in endotoxin-induced localized inflammatory hyperalgesia. Br. J. Pharmacol. **121**, 1619–1626
23 Mitchell, J. A., Akarasereennont, P., Themermann, C., Flower, R. J. and Vane, J. R. (1993) Selectivity of non-steroidal anti-inflammatory drugs as inhibitors of constitutive and inducible cyclo-oxygenase. Proc. Natl. Acad. Sci. U.S.A. **89**, 11693–11697

Received 11 September 2000/4 December 2000; accepted 24 January 2001

24 Sen, R. and Baltimore, D. (1986) Inducibility of kappa immunoglobulin enhancer-binding protein NF-κB by a posttranslational mechanism. Cell **46**, 705–716
25 Baines, D. L., Ramminger, S. J., Collet, A., Haddad, J. J. E., Best, O. G., Olver, R. E., Land, S. C. and Wislon, S. M. (2001) Oxygen-evoked electrogenic Na^+ transport in foetal distal lung epithelium. J. Physiol. (London), in the press
26 Ghosh, S. and Baltimore, D. (1990) Activation *in vitro* of NF-κB by phosphorylation of its inhibitor IκB. Nature (London) **344**, 678–682
27 Haddad, J. J. E. and Land, S. C. (2000) The differential expression of apoptosis factors in the alveolar epithelium is redox sensitive and requires NF-κB (RelA)-selective targeting. Biochem. Biophys. Res. Commun. **271**, 257–267
28 DiDonato, J. A., Hayakawa, M., Rothwarf, D. M., Zandi, E. and Karin, M. (1997) A cytokine-responsive IκB kinase that activates the transcription factor NF-κB. Nature (London) **388**, 548–554
29 Tsatmali, M., Graham, A., Szatkowski, D., Ancans, J., Manning, P., McNeil, C. J., Graham, A. M. and Thody, A. J. (2000) Alpha-melanocyte-stimulating hormone modulates nitric oxide production in melanocytes. J. Invest. Dermatol. **114**, 520–526
30 Taherzadeh, S., Sharma, S., Chhajlani, V., Gantz, I., Rajora, N., Demitri, M. T., Kelly, L., Zhao, H., Ichiyama, T., Catania, A. and Lipton, J. M. (1999) Alpha-MSH and its receptors in regulation of tumour necrosis factor-alpha production by human monocyte/macrophages. Am. J. Physiol. **276**, R1289–R1294
31 Huang, Q.-H., Hruby, V. J. and Tatro, J. B. (1998) Systemic alpha-MSH suppresses LPS fever via central melanocortin receptors independently of its suppression of corticosterone and IL-6 release. Am. J. Physiol. **275**, R524–R530
32 Chiao, H., Kohda, Y., McLeory, P., Craig, L., Housni, I. and Star, R. A. (1997) Alpha-melanocyte-stimulating hormone protects against renal injury after ischemia in mice and rats. J. Clin. Invest. **99**, 1165–1172
33 Chiao, H., Foster, S., Thomas, R., Lipton, J. and Star, R. A. (1996) Alpha-melanocyte-stimulating hormone reduces endotoxin-induced liver inflammation. J. Clin. Invest. **97**, 2038–2044
34 Haycock, J. W., Wagner, M., Morandini, R., Ghanem, G., Rennie, I. G. and Neil, S. M. (1999) Alpha-melanocyte-stimulating hormone inhibits NF-κB activation in human melanocytes and melanoma cells. J. Invest. Dermatol. **113**, 560–566